Adaptive Pontryagin's Minimum Principle-Inspired Supervised-Learning-based Energy Management for Hybrid Trains Powered by Fuel Cells and Batteries

Hujun Peng[1], Feifei Li[2], Zhu Chen[1], Kai Deng[1], Sebina Jeschke[2], Kay Hameyer[1]
1. Institute of Electrical Machines (IEM)
2. Institute for Information Management in Mechanical Engineering (IMA)
RWTH Aachen University
Aachen, Germany
Email: hujun.peng@iem.rwth-aachen.de
URL: https://www.iem.rwth-aachen.de/go/id/poti/?lidx=1

Acknowledgments

This study is funded by the German Federal Ministry of Transport and Digital Infrastructure (BMVi) under the National Innovation Program Hydrogen and Fuel Cell Technology (NIP). The funding numbers are 03B10502B and 03B10502B2. The authors gratefully thank the support of Siemens AG, Ballard, and NIP.

Keywords

≪Fuel Cell Electric Vehicle (FCEV)≫, ≪Energy System Management≫, ≪Neural Network≫

Abstract

This work develops a supervised learning-based strategy using Long Short-Term Memory Networks (LSTMN) to distribute power between fuel cells and batteries for fuel cell trains. The learning-based strategy exceeds the adaptive Pontryagin's minimum principle (PMP)-based strategy in all driving conditions, which is state-of-the-art. In the case with the most significant difference between the learning-based and the adaptive PMP-based strategy, more consumption of 1.84 % than the off-line PMP strategy, which determines the minimal hydrogen consumption for the same load profiles, is observed for the learning-based strategy. In comparison, 2.54 % more consumption is required by the adaptive PMP-based strategy compared to the off-line strategy.

Introduction

The world's first commercialized hybrid passenger train powered by fuel cells is developed by Alstom and began its operation in Germany in 2018, whose energy source system consists of batteries and proton-exchange membrane (PEM) fuel cells. Since the power change rate of fuel cell systems in hybrid vehicles is limited due to lifetime consideration, another battery system is required to cover the frequently varying load power in various driving conditions [1, 13]. Benefited from this kind of hybrid power source structure, the hydrogen usage efficiency of the hydrogen vehicles can be maximized by possibly optimal power distribution between fuel cells and batteries [14]. Many research works about energy management for hydrogen-powered vehicles are published in recent years, and some comprehensive reviews can be found in [3, 15]. The energy management strategies can be classified into three primary types: the rule-based method, the optimization-based method, and the learning-based method [4]. Developing the rule-based strategies and tuning their parameters are time-consuming, and the rule-based strategy is not optimal at the same time due to insufficient expertise.

The optimization-based methods are divided into global and local optimization-based methods. Furthermore, the global optimization-based energy management strategy is further classified into Pontryagin's Minimum Principle (PMP) as well as Dynamic Programming (DP). It has to be mentioned that the global optimization-based methods are off-line strategies as references to on-line strategies. For the local optimization-based power distribution methods, the most famous ones are the adaptive Pontryagin's Minimum Principle-based strategy (adaptive PMP) as well as the Equivalent Consumption Minimization Strategy (ECMS). Mathematically, ECMS can be obtained from the adaptive PMP because the equivalent factor defined in ECMS is linked to the co-state in the adaptive PMP [6]. The most crucial challenge faced with ECMS and the adaptive PMP is estimating the equivalent factor or the co-state [16, 17]. To our best knowledge, an analytical formula is proposed based on estimated mean values of fuel cell system power as well as the actual battery SoC values in [6] to estimate the co-state accurately and physically. However, the formula in [6] is based on average fuel cell power, and does not consider a so-called time effect. After checking the off-line PMP results, the co-state amplitude at the beginning of driving cycles is larger than that at the end. However, the formula in [6] calculates the same co-state values for the initial and end time point of the driving cycles. Therefore, this kind of sequence or time effect is not considered by the adaptive PMP method.

With machine learning technology developed, the learning-based strategies for hybrid vehicles attract more and more attention. The kind of sequence effect mentioned before can be taken into account by machine learning [8]. However, an enormous amount of data is required to train the learning-based method's control policy or prediction mechanism. Among the learning-based methods, the reinforcement learning is widely applied to develop energy management for hybrid vehicles in recent years [10]. Unlike the supervised learning, the reinforcement learning is a learning process of the policy principle by utilizing the interaction between agents and the environment under the pre-definition of a reward function. The advantage of reinforcement learning is that it can learn long-term accumulated rewards. However, for hybrid vehicles, its most significant drawback lies in the fact that the limited transferability of the trained control models. In this work, the long short-term memory network (LSTMN), as the most useful variant of RNN, is utilized to distribute load power for hybrid trains powered by fuel cells and batteries. Following contributions are included:

- The input variables are chosen based on the physical correlation between them and the output fuel cell power under the optimal control theory. Therefore, a small amount of data is required to train the learning-based strategy.
- After comparing the supervised-learning-based strategy to the off-line PMP strategy and the most energy efficient adaptive PMP-based strategies to our knowledge, a higher hydrogen usage efficiency than the adaptive PMP-based strategy is observed for the developed supervised-learning-based strategy.

Modeling of the serial hybrid powertrain

The entire drivetrain's configuration is displayed in Fig. 1. The fuel cell system *HD8* is supplied by the company *Ballard*, and it has a maximum net output power of 200 kW. The battery system has an energy capacity of about 200 kWh and a nominal voltage of 850 V, which can provide a maximal charge and discharge current of 900 A. The DC/DC converter is supplied by *Siemens*, which can provide a peak power of more than 1 MW and has a DC-link voltage of 1650 V.

The SoC of the entire battery system and the train speed are chosen as the state variables, while lookup tables are applied for modeling other subsystems' power losses. The exact models of each subsystem of the fuel cell train, as well as their related parameters, can be found in [6]. The altitude and speed profiles of three train lines are considered. The driving cycle 1 in Fig. 2a will be applied for training the neural network in the next section. The driving cycle 2 in Fig. 2b will be tested to validate the trained model, which comes from Regional Express 1 running between Aachen and Cologne. The driving cycle 3 in Fig. 2c corresponds to the Regional Express 27 running between Brandenburg and Berlin. This driving

cycle is an entire-day velocity trajectory of 19 hours and will be used for training or validation in an on-line simulation environment.

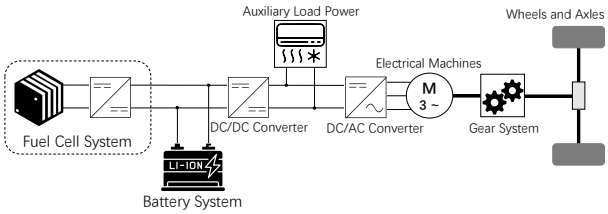

Fig. 1: Configuration of the serial hybrid drivetrain.

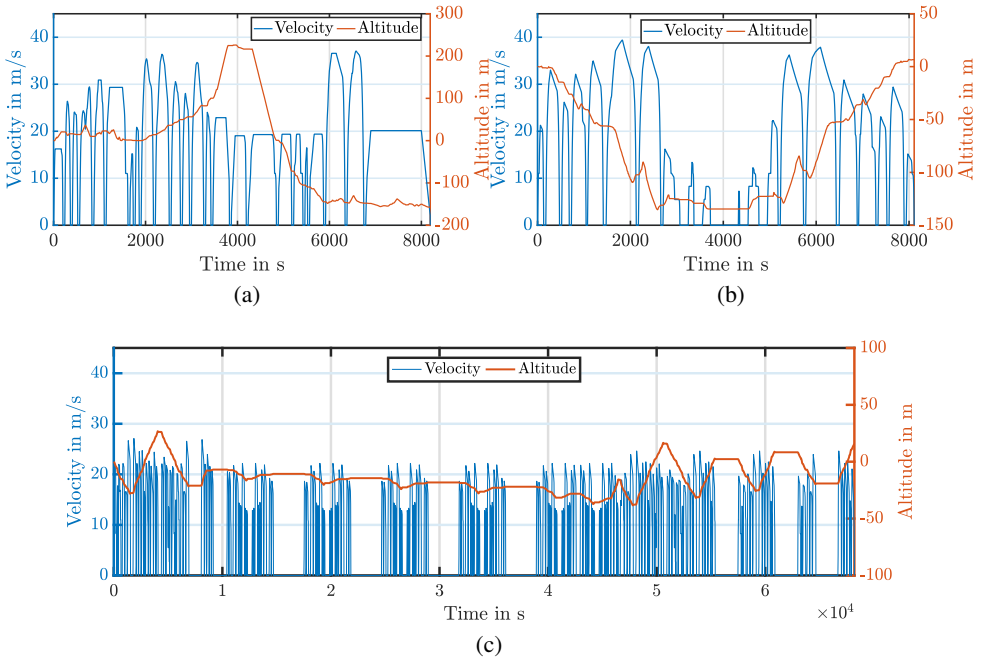

Fig. 2: Three driving cycles used in training and test: (a) Driving cycle 1 for training, (b) Driving cycle 2 for test, (c) Driving cycle 3 between Berlin and Brandenburg for training and test.

Machine learning-based strategies

This section consists of three parts: in the first part, the process of choosing input variables is explained, which has not been found in other works related to machine learning-based strategies for hybrid vehicles. In the second part, the LSTMN method is briefly introduced. Finally, in the third part, the training and test of models are displayed, and the most promising control block is prepared for validation in an on-line simulation environment in the next chapter. The whole process of developing the machine learning-based strategy is presented in Fig. 3.

Selection of input variables

The selection of input variables of the neural network is inspired by the adaptive PMP-based algorithm developed by the authors before. In [6], the adaptive PMP-based algorithm is described in detail. Therefore, a full review is not done here, and merely the process of choosing the input variables is explained. In the adaptive PMP-based strategy, the control variable is determined by minimizing the so-called Hamiltonian in every time instant as follows:

$$H(SoC(t), P_{\mathrm{fc}}(t), \lambda(t), t) = \dot{m}_{\mathrm{H_2}}(P_{\mathrm{fc}}(t)) + \lambda \cdot \dot{SoC}(t), \tag{1}$$

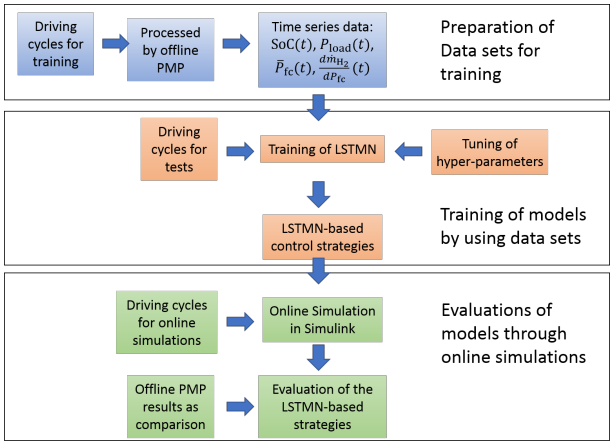

Fig. 3: Flow chart of developing the machine learning-based strategy, whereby the LSTMN method is used for the machine learning.

whereby $\dot{m}_{H_2}$ is the hydrogen mass flow mentioned before, and λ represents the co-state which is eventually a Lagrange factor. Then, by solving the following minimization problem, the optimal fuel cell power is determined in every time instant:

$$P_{fc}^{*}(t) = \underset{P_{fc}(t)}{\arg\min}(H(SoC(t), P_{fc}(t), \lambda(t), t)). \tag{2}$$

The estimation of the co-state is crucial for the performance of the adaptive PMP-based strategy. In [6], an analytic formula for estimating the co-state is derived from the energy conservation principle as follows:

$$\lambda = -V_{oc} \cdot Q \cdot \frac{d\dot{m}_{H_2}}{dP_{fc}}\bigg|_{P_{fc}=\overline{P}_{fc}}. \tag{3}$$

The battery capacity Q is assumed constant in this work. Then, according to (3), The mean value of fuel cell power and the battery open-circuit voltage V_{oc}, which is dependent on the SoC, influence mainly the co-state. After inserting (1) and (3) into (2), the control variable, namely the fuel cell power, depends on various inputs, including SoC, battery voltage, battery capacity, hydrogen consumption curves, average values of fuel cell power, demand load power as well as time.

The influence of the time or sequence effect on the output control variable is not apparent. In order to show the time effect, the co-state trajectories resulting from off-line PMP strategies for various driving cycles are demonstrated in Fig. 4. Thereby, the dependency of the co-state on SoC is presented. Furthermore, the estimated co-state by using the formula in (3) is also added. After comparison between the estimated co-state values and those resulting from off-line PMP, the average values of the co-state are well approximated by using the analytical formula (3). However, in the off-line PMP results, there are different co-state values at the same SoC. More precisely, the co-state amplitude near the end of the driving cycles is less than the initial co-state although they have the same SoC values and fuel cell system conditions. So far, the influence of the so-called time effect on the control variable is described. In order to have a control mechanism considering this kind of time effect, the LSTMN method will be used and explained in the next part.

Performance study of the LSTMN under different combinations of input variables

The training of the LSTMN requires the selection of features. The possible candidates of features include the open-circuit voltage V_{oc}, SoC, power demand P_{load}, average fuel cell power $\overline{P}_{fc}$, and the derivative of hydrogen mass flow with respective to the fuel cell power $\frac{d\dot{m}_{H_2}}{dP_{fc}}$ as well as the time. The control variable is the fuel cell power P_{fc}, which is also called the label in LSTMN. The training data sets correspond to the driving cycle 1, and the test of the trained model is applied to driving cycle 2. In the case of training

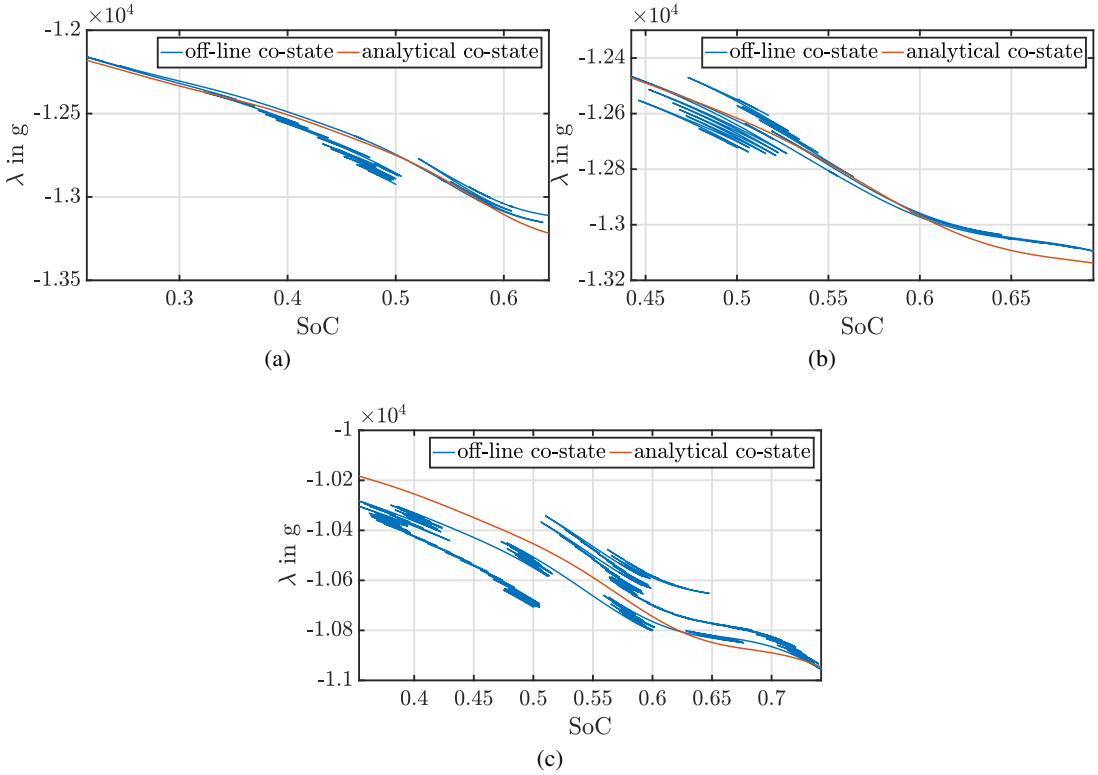

Fig. 4: Comparison between the analytically calculated co-state values and those resulting from off-line PMP algorithm under three different driving cycles: (a) Driving cycle 1 with average fuel cell power of 106.5 kW, (b) Driving cycle 2 with average fuel cell power of 114.1 kW, (c) Driving cycle 3 with average fuel cell power of 78.5 kW.

with more data, the data corresponding to driving cycle 3 is also used besides the driving cycle 1. In all experiments, the training data of the hybrid trains in summer and winter conditions are concatenated together. Before using the LSTMN, some parameter study for choosing best inputs combination will be implemented.

The first experiment aims to analyze which input combination performs best in predicting the label variable under test data sets. Numerical results are presented in Table I. The rMSE stands for root Mean Square Error in the field of machine learning, and MAE represents Mean Absolute Error. In above study

Table I: Performance study of the LSTMN under different inputs combinations.

Training inputs	rMSE (kW)	Training loss in MAE (kW)	Test loss in MAE (kW)
SoC + P_{load}	14.820	0.0094	0.0880
SoC + P_{load}+ V_{oc}	14.729	0.0093	0.0878
SoC + P_{load}+$\overline{P}_{\text{fc}}$ + V_{oc}	8.310	0.0066	0.0497
SoC + P_{load}+$\overline{P}_{\text{fc}}$ + V_{oc} + $\frac{d\dot{m}_{\text{H}_2}}{dP_{\text{fc}}}$	5.117	0.0062	0.0286
SoC + P_{load}+$\overline{P}_{\text{fc}}$ + V_{oc} + $\frac{d\dot{m}_{\text{H}_2}}{dP_{\text{fc}}}$ + Time	5.482	0.0065	0.0302

results, some conclusion can be made: P_{load} is the necessary input variable, $\overline{P}_{\text{fc}}$ is useful to set a baseline of season trend, and $\frac{d\dot{m}_{\text{H}_2}}{dP_{\text{fc}}}$ has positive influence on the prediction results. The time leads to a negative change in the trained model. As for adding the V_{oc}, the performance is not improved significantly, as the similar nature of SoC and V_{oc}, whereby the open-circuit voltage strongly depends on the SoC. In the following parts, more experiments are operated to explore their influences on the model. The numerical

results of the comparison are listed in Table II. Through the comparison study, a pretty close influence is generated between SoC and V_{oc} since their nature is similarly related in batteries. Given the rMSE results, the SoC has a slight advantage compared to V_{oc} in all three comparison experiments.

Table II: Comparative influence study between V_{oc} and SoC.

Training inputs	rMSE (kW)	Training loss in MAE (kW)	Test loss in MAE (kW)
V_{oc} + P_{load}+$\overline{P}_{fc}$	7.579	0.0071	0.0459
SoC + P_{load}+$\overline{P}_{fc}$	7.009	0.0068	0.0417
V_{oc} + P_{load}+$\overline{P}_{fc}$ + $\frac{d\dot{m}_{H_2}}{dP_{fc}}$	4.255	0.0062	0.0227
SoC + P_{load}+$\overline{P}_{fc}$ + $\frac{d\dot{m}_{H_2}}{dP_{fc}}$	4.175	0.0057	0.0225
V_{oc} + P_{load}+$\overline{P}_{fc}$ + $\frac{d\dot{m}_{H_2}}{dP_{fc}}$ + Time	5.384	0.0066	0.0306
SoC + P_{load}+$\overline{P}_{fc}$ + $\frac{d\dot{m}_{H_2}}{dP_{fc}}$ + Time	4.721	0.0061	0.0259

Due to the advantage of choosing SoC over the open-circuit voltage, the standard inputs are assigned as SoC, P_{load}, $\overline{P}_{fc}$ and $\frac{d\dot{m}_{H_2}}{dP_{fc}}$. The input of time is not explicitly further adopted because the performance of the trained model without an explicit input of time is better than that with time as the input.

After choosing the input variables, the fine-tuning experiments of hyper-parameters are implemented. This step tests if using more training data by utilizing driving cycle 3, changing the learning rate, and adding an early-stop policy influence the training and testing results. The fine-tuning results are expressed in Table III. From the results, the change of learning rate is illustrated as a strong influence factor, which is capable of improving the model's performance twofold.

While monitoring the training and test loss, as shown in Fig. 5, the over-fitting phenomenon are much more significant with more training data from driving cycle 3. Hence, the early stop policy is adopted when involving more training data by using driving cycle 3. The computational time takes about ten seconds to train one epoch by using a computer with *2.6 GHz 6Core Intel Core i7*. Since 50 epochs are used to train the neural network, it takes about five hundred seconds for a combination of input variables per a setup of hyper-parameters. The low computational time results from that merely one driving cycle is applied to train the neural network, and this driving cycle contains about 16000 sampled time points. Furthermore, the test results of the best two models in Table III, corresponding to the last two rows, are shown in Fig. 6, whereby negligible difference among models is observed.

Table III: Results of hyper-parameters fine tuning. Thereby, *lr* stands for the learning rate and more training data comes from driving cycle 3.

Methods	rMSE (kW)	Training loss in MAE (kW)	Test loss in MAE (kW)
Standard inputs / lr = 0.001	4.175	0.0057	0.0225
Standard inputs / lr=0.0001	2.213	0.0075	0.0114
Standard inputs / More training data / lr=0.0001	3.607	0.0051	0.0179
Standard inputs / lr=0.0001 / early stop	2.012	0.0078	0.0097
Standard inputs / More training data / lr=0.0001 / early stop	1.718	0.0047	0.0072

In the next section, the machine learning-based strategy's fuel economy will be validated by applying simulation. It is worth mentioning that the trained model includes four input signals: load power, SoC, fuel cell average power, and the derivative of the mass flow regarding the fuel cell output power. Furthermore, the training data set merely uses the driving cycle 1 to keep the training effort low, and the learning-based strategy will be tested under driving cycles 2 and 3 for different weather conditions in the on-line simulation environment.

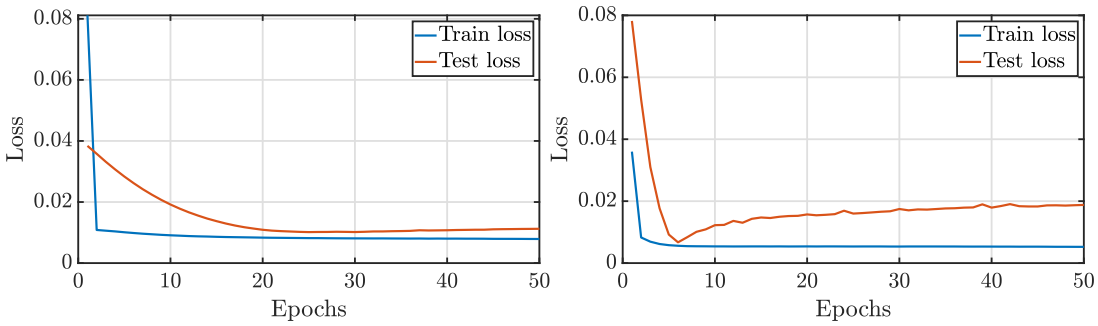

Fig. 5: Training loss and test loss monitoring: (a) Training process of standard inputs with learning rate equals 0.0001 and training data from driving cycle 1, (b) Training process of standard inputs with more training data from driving cycle 3 besides the data from driving cycle 1 at learning rate equals 0.0001.

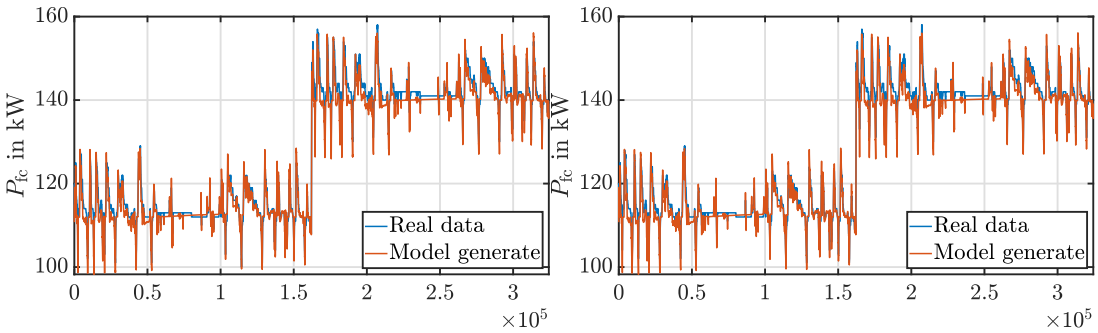

Fig. 6: Test results of the best two trained models, whereby driving cycle 2 is used for testing. In the legend, the *Real data* represents the control sequences under the off-line PMP strategy, and the *Model generate* is the output of the trained model. (a) The trained model with standard inputs and training data from driving cycle 1, (b) The trained model with standard inputs with training data from driving cycles 1 and 3.

On-line simulation results with comparisons to off-line and adaptive PMP strategies

In the on-line simulation environment, the learning-based strategy will be compared to the off-line PMP strategy to show how close the machine learning-based strategy is to the optimal strategy. Besides that, the learning-based strategy will be compared to the adaptive PMP-based strategy developed by authors before, which is the most fuel-efficient strategy so far, to our knowledge. The high fuel economy and adaptivity of the developed learning-based strategies will be emphasized through comparisons to either the off-line or on-line strategies.

It is worth mentioning that in the on-line simulation environment, the control signal from the energy management system, which is the fuel cell system power, suffers from a rate limit in order to reduce fuel cell aging, which is about 20 kW/s for a system with a maximum power of 200 kW. Furthermore, due to simplicity, this rate limit is set to be the same for increasing and decreasing fuel cell power. The charge and discharge current of the battery system is determined by the driving cycle because the battery system assists the train acceleration and regenerative braking. Due to the battery system's high power dynamic capability, there are no other rate limiters in the on-line simulation.

In Fig. 7a, the fuel cell power trajectories under the learning-based strategy are displayed, together with the off-line PMP results. The fuel power trajectories are close to their mean values to a large degree and

above the mean values during acceleration while below the average values in the regenerative braking phase. Therefore, the battery system provides and absorbs peak power during acceleration and regenerative braking phases, either under the machine learning-based strategy or the off-line PMP-based strategy, as shown in Fig. 7c. As the result of the battery power trajectories, the corresponding SoC trajectories can be found in Fig. 7b. It is worth mentioning that the change rate in the fuel cell power trajectories, corresponding to the acceleration and regenerative braking phases, adheres to the dynamic limits of the fuel cell power mentioned before. These acceleration and braking phases take more than one minute, and the variation in the fuel cell power is less than 40 kW. Regarding the fuel cell trajectories, the closeness of the trajectories to their mean values means utilizing the convexity of the hydrogen consumption curve, which enables working points of the fuel cell system with high efficiency. The increase of fuel cell power during acceleration and the decrease during regenerative braking help to reduce battery losses because the batteries cover the difference between load demand and supplied fuel cell power. Thereby, an oscillation of fuel cell power, to some degree, helps reduce battery current, ohmic losses, and total hydrogen consumption. Therefore, a compromise between maintaining the fuel cell system in operational points with high efficiency and reducing inner battery losses has to be met to reduce the total hydrogen consumption. After comparing the off-line PMP strategy, which realizes the best fuel economy, it is evident that the machine learning-based strategy can work close to the best compromise and leads to good fuel economy. In Fig. 7b, the SoC trajectory has an end value close to its initial value, which shows that the charge-sustaining mode is maintained for the fuel cell trains without an extra charger. Regarding hydrogen consumption, the learning-based strategy consumes 1.84 % more compared to the off-line PMP strategy in summer for driving cycle 3.

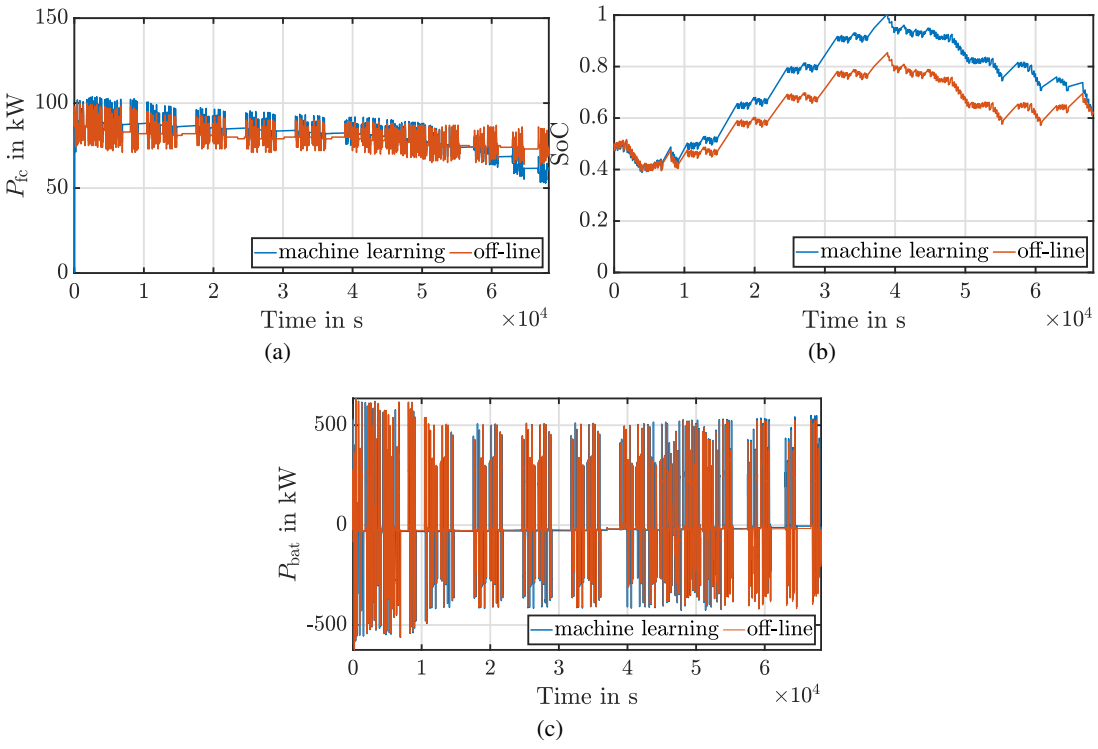

Fig. 7: On-line simulation results under the learning-based strategy for driving cycle 3 in summer with the off-line optimal results as references: (a) Fuel cell power trajectories, (b) SoC trajectories, (c) Battery power trajectories.

The validation is also performed for the winter weather conditions. Moreover, the difference between the learning-based strategy and the off-line PMP strategy decreases in winter conditions compared to the difference in summer because a higher average load demand power is estimated with lower relative errors. The fuel cell power trajectories are also close to their average values, which are about 30 kW larger than in summer, and the SoC trajectories are also similar to the cases in summer since the higher

auxiliary consumption due to air conditioning will be covered by the fuel cell system. Regarding hydrogen consumption, the learning-based strategy consumes 1.58 % more than the off-line strategy in winter for driving cycle 3.

The validation of the fuel economy of the learning-based strategy, with comparison to the off-line strategies, is also done for driving cycle 2 and different weather conditions. Some related parameters to fuel economy can be found Table IV.

Besides comparing the learning-based strategy and the off-line PMP, another comparison will be given between the learning-based strategy and the adaptive PMP-based strategy since this work aims to develop a strategy better than the best adaptive PMP-based strategy known so far. The comparison between them is carried under driving cycle 3 in summer weather conditions.

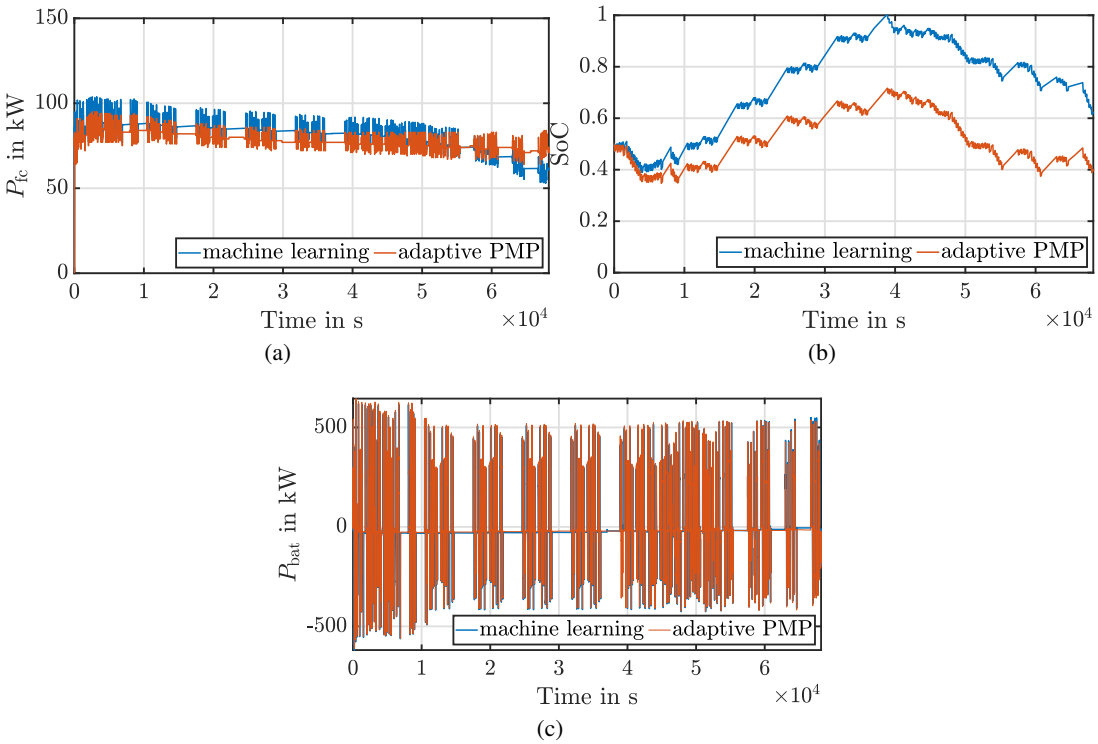

Fig. 8: Comparison of the learning-based strategy and the adaptive PMP-based strategy under driving cycle 3 in summer weather conditions: (a) Fuel cell trajectories, (b) SoC, (c) Battery power trajectories.

The resulting trajectories, which make the learning-based strategy different from the adaptive PMP-based strategy, can be found under the driving cycle 3 with a longer running time. The battery power trajectories of the learning-based strategy and the adaptive PMP-based strategy, as shown in Fig. 8c, are slightly different. In Fig. 8a and Fig. 8b, more differences regarding the fuel cell power and SoC trajectories can be identified. The fuel cell power under the learning-based strategy has a higher average value than that under the adaptive PMP-based strategy in the beginning and midterm of the driving cycle, while near the end of driving cycle 3, the fuel cell power under the learning-based strategy is less than that of the adaptive PMP-based strategy. In other words, under the learning-based strategy, more fuel cell power than the estimated average power will be used at the beginning of the driving cycle and less fuel cell power than the estimated average power used near the end of the driving cycle. This phenomenon is similar to the time or sequence effect mentioned before, whereby in the off-line PMP, the same SoC values correspond to different co-state values due to different time points within driving cycles. More detailed to speak, the amplitude of the co-state at the beginning of the driving cycle is larger than that near the end of the driving cycle, even though the same SoC values exist. Due to the larger co-state amplitude at the beginning of the driving cycle, the off-line PMP strategy outputs fuel cell power more than its average first and decreases the power later less than its average. Therefore, it is evident that the learning-based strategy

can consider the time or sequence effect to minimize hydrogen consumption. A simple explanation of the benefits of considering this kind of time or sequence effect follows. Due to the difference in fuel cell power, the SoC trajectory under the learning-based strategy lies in higher values than the adaptive PMP-based strategy, as shown in Fig. 8b. According to the battery characteristics, a higher SoC results in a higher open-circuit voltage and lower battery resistance. Then, for the same battery power, a lower battery current and inner ohmic losses result. As mentioned before, the basic principle of minimizing hydrogen consumption for fuel cell trains lies in the compromise between maintaining the fuel cell system working at higher efficiency and reducing inner battery losses. By considering this kind of time or sequence effect in the learning-based strategy, the battery losses will be further decreased.

The comparison between the learning-based strategy and the adaptive PMP-based strategy is also done for driving cycle 2 and other weather conditions. The results can be found in Table IV. Summarily, the

Table IV: Comparison of the learning-based strategy and the adaptive PMP-based strategy with off-line PMP as references.

		Driving cycle 2		Driving cycle 3	
		Summer	Winter	Summer	Winter
	m_{H_2} in g	15599	20843	87589	120379
	m_{H_2} in g under PMP	15200	20339	86007	118504
Learning-based	Compared to PMP	2.63 %	2.48 %	1.84 %	1.58 %
	m_{H_2} in g	15617	20862	84954	120390
	m_{H_2} in g under PMP	15195	20349	82847	118486
Adaptive PMP	Compared to PMP	2.78 %	2.52 %	2.54 %	1.61 %

most important results of the supervised-learning-based strategy, with comparisons to the off-line PMP and the on-line adaptive PMP-based strategies, are included in Table IV. The learning-based strategy has a higher fuel economy than the adaptive PMP-based strategy in all driving conditions, independent of the length of driving cycles and weather conditions. The reason is that the learning-based strategy considers the time or sequence effect, besides all the merits included in the adaptive PMP-based strategy.

Conclusions

In this work, a learning-based strategy is developed using LSTMN, a variant of the recurrent neural network, to distribute power between fuel cells and batteries for fuel cell trains. The inputs of the neutral network are chosen based on inspiration from the adaptive PMP-based strategy. Due to their physical relation to the output fuel cell power, much less data is required to train the learning-based strategy than those in the literature about learning-based strategies. Based on simulation results, the learning-based strategy outperforms the best adaptive PMP strategy, which is the best strategy to our knowledge, in all driving conditions. In the case with the most significant difference between the learning-based and the adaptive PMP-based strategy, more consumption of 1.84 % compared to the off-line PMP results for the learning-based strategy for a typical driving cycle of regional trains in summer, while 2.54 % more consumption is required by the adaptive PMP strategy than the off-line PMP strategy for the same driving cycle.

References

[1] Fletcher, T. and Ebrahimi, K., 2020. The effect of fuel cell and battery size on efficiency and cell lifetime for an L7e fuel cell hybrid vehicle. Energies, 13(22), p.5889

[2] Lü, X., Wu, Y., Lian, J., Zhang, Y., Chen, C., Wang, P. and Meng, L., 2020. Energy management of hybrid electric vehicles: A review of energy optimization of fuel cell hybrid power system based on genetic algorithm. Energy Conversion and Management, 205, p.112474

[3] Sulaiman, N., Hannan, M.A., Mohamed, A., Ker, P.J., Majlan, E.H. and Daud, W.W., 2018. Optimization of energy management system for fuel-cell hybrid electric vehicles: Issues and recommendations. Applied energy, 228, pp.2061-2079
[4] Peng, H., Chen, Z., Deng, K., Dirkes, S., Ünlübayir, C., Thul, A., Löwenstein, L., Sauer, D.U., Pischinger, S. and Hameyer, K., 2021. A comparison of various universally applicable power distribution strategies for fuel cell hybrid trains utilizing component modeling at different levels of detail: From simulation to test bench measurement. eTransportation, 9, p.100120
[5] Peng, H., Chen, Z., Li, J., Deng, K., Dirkes, S., Gottschalk, J., Ünlübayir, C., Thul, A., Löwenstein, L., Pischinger, S. and Hameyer, K., 2021. Offline optimal energy management strategies considering high dynamics in batteries and constraints on fuel cell system power rate: From analytical derivation to validation on test bench. Applied Energy, 282, p.116152
[6] Peng, H., Li, J., Löwenstein, L. and Hameyer, K., 2020. A scalable, causal, adaptive energy management strategy based on optimal control theory for a fuel cell hybrid railway vehicle. Applied Energy, 267, p.114987
[7] Chen, Z., Liu, Y., Ye, M., Zhang, Y. and Li, G., 2021. A survey on key techniques and development perspectives of equivalent consumption minimisation strategy for hybrid electric vehicles. Renewable and Sustainable Energy Reviews, 151, p.111607
[8] Li, W., Cui, H., Nemeth, T., Jansen, J., Ünlübayir, C., Wei, Z., Zhang, L., Wang, Z., Ruan, J., Dai, H. and Wei, X., 2021. Deep reinforcement learning-based energy management of hybrid battery systems in electric vehicles. Journal of Energy Storage, 36, p.102355
[9] Zhou, D., Ravey, A., Al-Durra, A. and Gao, F., 2017. A comparative study of extremum seeking methods applied to online energy management strategy of fuel cell hybrid electric vehicles. Energy conversion and management, 151, pp.778-790
[10] Tan, H., Zhang, H., Peng, J., Jiang, Z. and Wu, Y., 2019. Energy management of hybrid electric bus based on deep reinforcement learning in continuous state and action space. Energy Conversion and Management, 195, pp.548-560
[11] Han, L., Jiao, X. and Zhang, Z., 2020. Recurrent neural network-based adaptive energy management control strategy of plug-in hybrid electric vehicles considering battery aging. Energies, 13(1), p.202
[12] Munoz, P.M., Correa, G., Gaudiano, M.E. and Fernández, D., 2017. Energy management control design for fuel cell hybrid electric vehicles using neural networks. International Journal of Hydrogen Energy, 42(48), pp.28932-28944
[13] Kandidayeni, M., Trovo, J.P., Soleymani, M. and Boulon, L., 2022. Towards health-aware energy management strategies in fuel cell hybrid electric vehicles: A review. International Journal of Hydrogen Energy.
[14] Manoharan, Y., Hosseini, S.E., Butler, B., Alzhahrani, H., Senior, B.T.F., Ashuri, T. and Krohn, J., 2019. Hydrogen fuel cell vehicles; current status and future prospect. Applied Sciences, 9(11), p.2296.
[15] Ahmadi, S., Bathaee, S.M.T. and Hosseinpour, A.H., 2018. Improving fuel economy and performance of a fuel-cell hybrid electric vehicle (fuel-cell, battery, and ultra-capacitor) using optimized energy management strategy. Energy Conversion and Management, 160, pp.74-84.
[16] Li, H., Ravey, A., NDiaye, A. and Djerdir, A., 2019. Online adaptive equivalent consumption minimization strategy for fuel cell hybrid electric vehicle considering power sources degradation. Energy Conversion and Management, 192, pp.133-149.
[17] Musardo, C., Rizzoni, G., Guezennec, Y. and Staccia, B., 2005. A-ECMS: An adaptive algorithm for hybrid electric vehicle energy management. European journal of control, 11(4-5), pp.509-524.